

Received: 2020.12.27

Accepted: 2020.05.14

Available online: 2020.06.20

Published: 2020.08.21

# Involvement of p53, p21, and Caspase-3 in Apoptosis of Coronary Artery Smooth Muscle Cells in a Kawasaki Vasculitis Mouse Model

Authors' Contribution:  
Study Design A  
Data Collection B  
Statistical Analysis C  
Data Interpretation D  
Manuscript Preparation E  
Literature Search F  
Funds Collection G

ACE 1 **Minghong Deng**  
AE 1 **Chunwang Lin**  
C 1 **Xianglin Zeng**  
BD 1 **Jianping Zhang**  
C 1 **Fang Wen**  
B 2 **Ziguang Liu**  
B 3 **Haiyan Wu**  
B 4 **Xiaofeng Wu**

1 Pediatric Intensive Care Unit, Shunde Women and Children's Hospital of Guangdong Medical University, Foshan, Guangdong, P.R. China  
2 Pathological Department, Shunde Women and Children's Hospital of Guangdong Medical University, Foshan, Guangdong, P.R. China  
3 Inspection Department, Shunde Women and Children's Hospital of Guangdong Medical University, Foshan, Guangdong, P.R. China  
4 Inspection Department, Guangzhou Jinyu Medical Examination Center, Guangzhou, Guangdong, P.R. China

**Corresponding Author:** Chunwang Lin, e-mail: 1933500933@qq.com

**Source of support:** This study was supported by the Science Department of Foshan City in China (Grant No. 2015AB002413)

**Background:** Overexpression of p53, p21, and caspase-3 promotes apoptosis of vascular smooth muscle cells. However, the mechanisms that lead to apoptosis of coronary artery smooth muscle cells (CASMCs) is unclear in Kawasaki disease (KD). This study investigated involvement of p53, p21, and caspase-3 in the apoptosis of CASMCs from a Kawasaki vasculitis mouse model.

**Material/Methods:** The Kawasaki vasculitis mouse model with coronary artery lesions was generated via administration of *Lactobacillus casei* cell wall extract. In 2 groups of mice (healthy control and KD vasculitis mice), the levels of p53, p21, and caspase-3 protein in the root of the coronary artery were evaluated via immunohistochemistry. Receiver operating characteristic curves were plotted for determination of area under the curve, 95% confidence interval, sensitivity, specificity, and cutoff values for the ability of p53, p21, and caspase-3 expression to predict CASMC apoptosis and coronary artery lesion formation in KD vasculitis mice.


**Results:** Compared with healthy mice, KD vasculitis mice had a significantly higher apoptosis index and upregulated p53, p21, and caspase-3 expression. Also, the immunoreactive score for caspase-3 was positively correlated with the immunoreactivity scores for p53 and p21. The optimal cutoff values for p53, p21, and caspase-3 expression for predicting the presence of coronary artery lesions were 4.15, 4.18, and 4.22, respectively.

**Conclusions:** Upregulated levels of p53, p21, and caspase-3 promoted apoptosis of CASMCs in KD vasculitis mice. Thus, the levels of p53, p21, and caspase-3 may serve as valuable predictors of coronary artery lesion formation in KD.

**MeSH Keywords:** **Apoptosis • Coronary Vessels • Mucocutaneous Lymph Node Syndrome**

**Abbreviations:** **CASMC** – coronary artery smooth muscle cell; **KD** – Kawasaki disease; **CI** – confidence interval; **AUC** – area under the curve; **ROC** – receiver operating characteristic; **IRS** – immunoreactive score; **CAL** – coronary artery lesions; **AAA** – abdominal aortic aneurysm; **SMC** – smooth muscle cells; **PBS** – phosphate-buffered saline; **AI** – apoptosis index; **HRP** – horseradish peroxidase; **PARP** – poly ADP-ribose polymerase

**Full-text PDF:** <https://www.medscimonit.com/abstract/index/idArt/922429>

 2788

 2

 5

 20



## Background

Kawasaki disease (KD) is a rare disease but a primary cause of posterior heart disease occurring in preschool children [1]. Clinically, KD is manifested as inflammation of blood vessels (i.e., vasculitis) throughout the body, and it thus involves a variety of organs and tissues, including the coronary arteries [2,3]. The most significantly affected vascular site is the root near the opening of the coronary artery [2]. Coronary artery lesions (CALs) are characterized by a narrowing or dilation of the lumen of the coronary artery due to nonspecific inflammation [4,5]. Some CALs lead to the rupture of coronary artery aneurysms or cause coronary arterial stenosis and ischemia, all of which may result in unfavorable outcomes such as myocardial infarction [4–6]. The mechanisms underlying the pathogenesis of CAL remain unclear. However, Lopez-Candales et al. [7] showed that the pathological changes in abdominal aortic aneurysm (AAA) cases include apoptosis of smooth muscle cells (SMCs), which is related to the overexpression of p53 in these cells, suggesting that p53 plays an important role in SMC apoptosis. In addition, B-cell lymphoma 2 (Bcl2) is a well-known apoptotic suppressor [8], whereas cysteine aspartic acid protease 3 (caspase-3) is a pro-apoptotic gene [9]. Previous studies suggested that Bcl-2 and caspase-3 play key roles in apoptosis in general [8–10]. Hence, it is reasonable to hypothesize that the pathological changes in CALs of KD may be similar to those observed in AAA, both of which are examples of vascular plasticity characterized by SMC apoptosis in the artery wall [7]. However, the pathogenesis of apoptosis of coronary artery smooth muscle cells (CASMCs) has not been elucidated, and whether changes in the expression levels of p21, p53, and caspase 3 are correlated with the induction of CASMC apoptosis in KD remains unclear.

In this study, we generated a KD vasculitis mouse model and researched the roles of p21, p53, and caspase-3 in the apoptosis of CASMCs in KD vasculitis mice and their correlation. We also assessed the ability of p21, p53, and caspase-3 expression to predict the presence of CALs in KD vasculitis mice. Our study provides direct evidence that increased expression levels of p21, p53, and caspase 3 are implicated in the development of CASMC apoptosis and these factors may be valuable predictors of CAL formation in KD.

## Material and Methods

The animal experiments were approved by the Ethics Committee of Shunde Women and Children's Hospital of Guangdong Medical University (Protocol Number: 2016002). All operations were performed after animals were anesthetized with pentobarbital to prevent suffering.

## Generation of KD vasculitis mice

Mice were from the Guangdong Medical Laboratory Animal Center (Guangzhou, China; License number, SCXK (Guangdong) 2013-0034), and housing and feeding were standardized [11]. Twenty-four male BALB/c mice (4–6 weeks old, weighing 20–25 g) were used in the study. These mice were randomly divided into a KD group (n=12) and a control group (n=12). To induce KD coronary vasculitis, 500 µg of cell wall extract from *Lactobacillus casei* (CICC 6105; The China Center of Industrial Culture Collection, Beijing, China) was injected into each BALB/c mouse in the KD group [11,12]. All mice were maintained for 14 days before sacrifice and harvesting of the hearts for analysis. The mice of the control group received a placebo injection.

## Specimen collection and apoptosis evaluation

Mice were anesthetized, and sterile thoracotomy was performed to collect the heart and blood vessels, which were placed in a precooled D-Hank's culture dish. The left and right coronary arteries of the heart were parted using ophthalmic scissors, and root tissue was cut. Four percent paraformaldehyde was used to fix the root tissue, which was then dehydrated and embedded in paraffin. Continuous 6-µm cross-sectional slices were produced, with each part of a blood vessel being sectioned 10 times and stained with hematoxylin-eosin (H&E) according to the standard H&E staining protocol.

The pathological changes in coronary root tissues were assessed as follows. Five randomly selected non-overlapping high-power microscopic fields (×40) were randomly selected for counting and scoring the number of apoptosis-positive nuclei and the total number of nuclei. Image-Pro Plus 4.5 (Media Cybernetics, Silver Spring, MD, USA) was used to calculate the apoptosis index (AI) of CASMCs (AI=number of apoptotic nuclei/total number of nuclei × 100%).

## Reagents

The following antibodies were obtained from Beijing Zhongshan Jinqiao Biotechnology, Inc. (Beijing, China): rabbit polyclonal anti-bcl-2 and anti-caspase-3 antibodies, mouse monoclonal anti-p53 and anti-p21 antibodies, and horseradish peroxidase (HRP) – polymer linkage anti-mouse antibody.

## Immunohistochemistry

The tissues were fixed in 4% paraformaldehyde, sequentially dehydrated, paraffin-embedded, and sectioned to generate 4-µm-thick slides. For immunostaining, briefly, sections underwent an antigen high-pressure repair and endogenous peroxidase treatment and were then incubated with a mouse anti-monoclonal primary antibody (1: 100 dilution) at 4°C overnight.

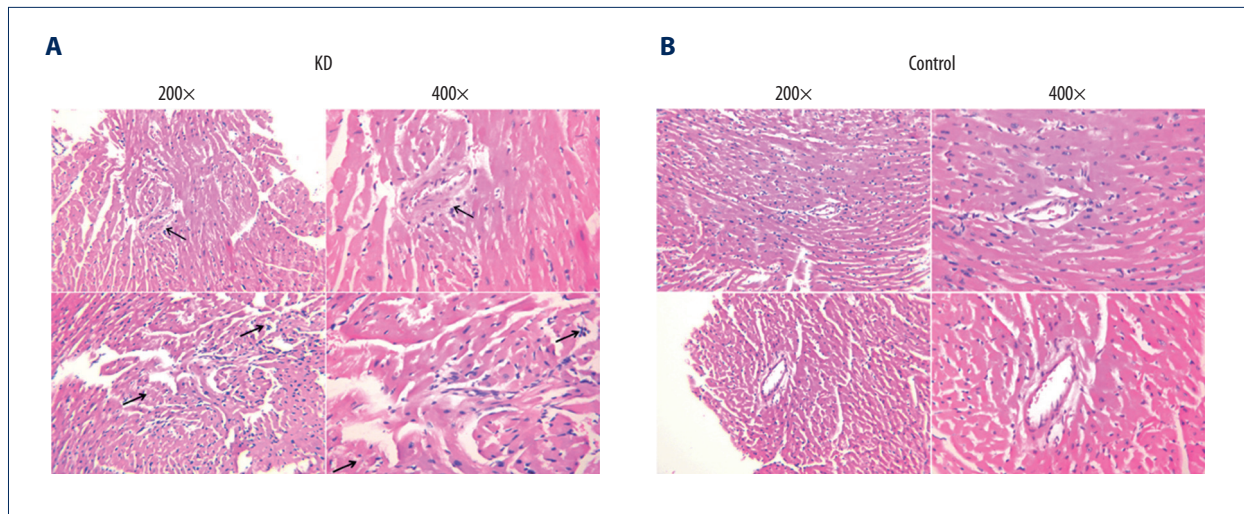


**Figure 1.** Pathological features of the coronary artery root in KD (A) and control (B) groups. The root of the coronary artery obtained from the KD vasculitis mice exhibited accumulation of foam cells and inflammatory cell infiltration, which were accompanied by dissolved and necrotic CASMCs, as arrows pointing to the positions. These pathological phenotypes were not present in the coronary artery of the control mice.

Next, dry slides were washed with PBS and incubated with an HRP polymer-bonded secondary antibody for 60 min. The specific staining was visualized with the substrate chromogen. Negative controls were performed in the absence of primary antibody. The slides were sealed with neutral gum.

### Immunoreactivity score of CASMCs

Two independent pathologists who were blinded to the pathological data respectively scored the immunostaining intensity. Any discrepancy in the scores obtained by the 2 pathologists were resolved through reassessment. The immunolabeling of CASMCs was assessed. Five fields were randomly selected, and the number and the percentage of positively stained cells were computed. According to the antibody specification, to determine whether cytoplasmic staining was positive or negative, semiquantitative scoring based on the intensity of each sample was carried out using a previously reported method [13, 14]. The staining intensity was stratified as follows: 0 indicated no staining; 1, mild staining; 2, moderate staining; and 3, strong staining. The percentage scoring of CASMCs was stratified as follows: 0% (score=0), 1–10% (score=1), 11–50% (score=2), 51–75% (score=3), and >75% (score=4). In order to obtain semiquantitative expression data of staining intensity of CASMCs and carry out an accurate statistical analysis, the final immunoreactivity scores (IRS) of each sample was determined by adding the 2 score values for the immunostaining intensity and the immunostaining percentage.

### Statistical analyses

The statistical analyses were performed with SPSS version 17.0 statistical software (SPSS Software, Chicago, IL, USA). Graphs

and receiver operating characteristic (ROC) curves were generated using GraphPad software (GraphPad Software, La Jolla, CA, USA). The chi-squared test was used for comparisons of the positive rates of p53 and p21 expression and the CASMC AIs between the KD and the control groups. Student's *t*-test was applied for comparisons of the IRS values for p53, p21, Bcl2, and caspase-3 between the KD and the control groups. Pearson's test was applied for the correlation of p53, p21, and caspase-3 IRSs with CASMC apoptosis in KD vasculitis mice. ROC curves were employed to determine the optimal cutoff values for p53, p21, and caspase-3 expression for predicting the development of CASMC apoptosis and CAL formation in KD vasculitis mice, and to determine the values for the ROC area under the curve (AUC), 95% confidence interval (CI), sensitivity, specificity, and positive likelihood ratio. Significance was established at the level of  $P < 0.05$ .

## Results

### Increased apoptosis of CASMCs in KD vasculitis mice

We generated KD vasculitis mice with CALs as previously described [11,12]. Between the control and KD groups, we did not see any significant differences in body weight during the 30-day study period ( $t=1.02$ ,  $P > 0.05$ ). Histological examination revealed that the root of the coronary artery obtained from the KD vasculitis mice exhibited an accumulation of foam cells and inflammatory cell infiltration, which were accompanied by dissolved and necrotic CASMCs. Meanwhile, the middle layer of the coronary artery was thickened, with actively proliferating fibroblasts in the vascular wall and broken elastic



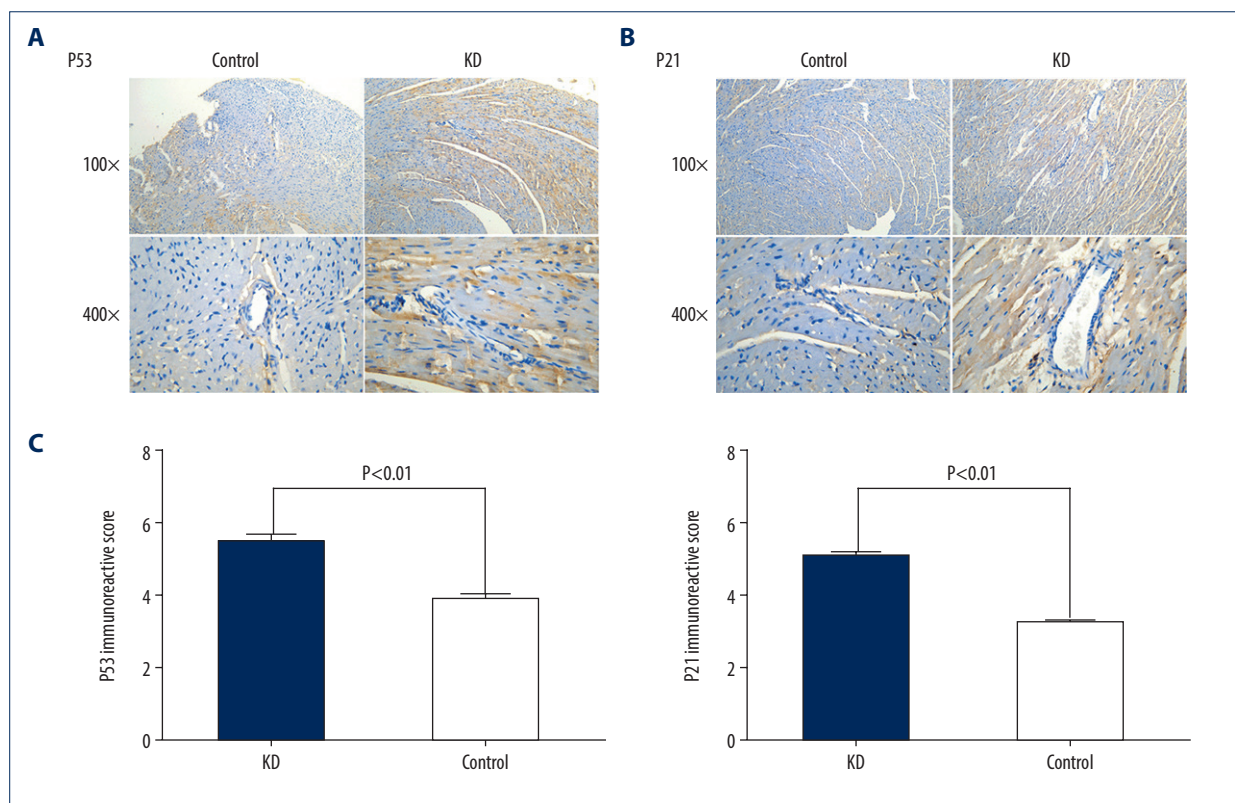


**Figure 2.** Comparison of p53 (A, C) and p21 (B, C) IRS values between the KD (n=12) and control groups (n=12). Cytoplasmic staining of p53 in CASMCs was moderate and strong in the mice of the KD group, whereas only mild or no staining was observed in mice of the control group (A). Cytoplasmic staining for p21 in CASMCs was moderate and strong in mice of the KD group, but mild or absent in mice of the control group (B). The IRS values for p53 and p21 were significantly different between the KD group and control group (C).

fibers (Figure 1A). These pathological phenotypes were not present in the coronary artery of the control mice (Figure 1B). These phenotypic characteristics indicated successful establishment of the KD vasculitis mouse model in this study. We next compared the apoptosis rate in the root of the coronary artery between the control and KD groups as evaluated by AI values. The AI of CASMCs in KD vasculitis mice was  $35.47 \pm 8.62$ , which was greater than that of CASMCs in control mice ( $4.51 \pm 1.12$ ;  $\chi^2=7.25$ ,  $P<0.001$ ), suggesting increased apoptosis in the coronary artery of KD vasculitis mice.

#### Increased expression of apoptotic factors in KD vasculitis mice

Given the increased apoptosis in the root of the coronary artery of KD vasculitis mice, we next assessed the expression of several well-defined apoptotic factors including p53 and p21 by immunohistochemistry. The percentages of cells stained positively for p53 and p21 in the coronary artery of KD vasculitis mice were 60% and 65%, respectively, in the KD group, compared with 25% and 20%, respectively, in the control group ( $\chi=3.56$  and  $\chi=3.97$ , all  $P<0.001$ ). Cytoplasmic staining of p53

in CASMCs was moderate in 75% of mice (n=9) and strong in 25% of mice (n=3) in the KD group compared with mild staining in 83.33% of mice (n=10) and no staining in 16.67% of mice (n=2) in the control group. Cytoplasmic staining for p21 in CASMCs was moderate in 66.67% of mice (n=8) and strong in 33.33% of mice (n=4) in the KD group compared with mild staining in 75% of mice (n=9) and no staining in 25% of mice (n=3) in the control group. In the KD group, the IRS values for p53 and p21 were  $5.33 \pm 0.90$  and  $6.37 \pm 0.76$ , respectively, compared with  $4.05 \pm 1.05$  and  $4.43 \pm 0.51$ , respectively, in the control group ( $t=4.61$  and  $5.30$ ;  $P=0.001$  and  $0.001$ ; Figure 2A–2C; Table 1). These results show that KD vasculitis mice had increased expression of p53 and p21, uniform with the observed increase in apoptosis.

In addition, the percentages of cells stained positively for Bcl2 and caspase-3 were 25% and 80%, respectively, in the KD group, compared with 70% and 20% in the control group ( $\chi=3.94$  and  $\chi=5.27$ , all  $P<0.001$ ). Cytoplasmic staining for Bcl2 in CASMCs was mild in 66.67% of mice (n=8) and not observed in 33.33% of mice (n=4) in the KD group compared with strong staining in 83.33% of cells (n=10) and moderate staining in 16.67% of

**Table 1.** Comparison of IRS values for p53, p21, Bcl2, and caspase-3 between the KD and control groups.

Group	n	p53 IRS	p21 IRS	Bcl2 IRS	Caspase-3 IRS
KD	12	5.33±0.90	5.07±0.70	4.43±0.51	5.60±0.50
Control	12	4.05±1.05	3.21±0.97	6.37±0.76	3.83±0.38
<i>t</i>		4.61	5.30	5.79	5.24
<i>P</i>		0.001	0.001	0.001	0.001

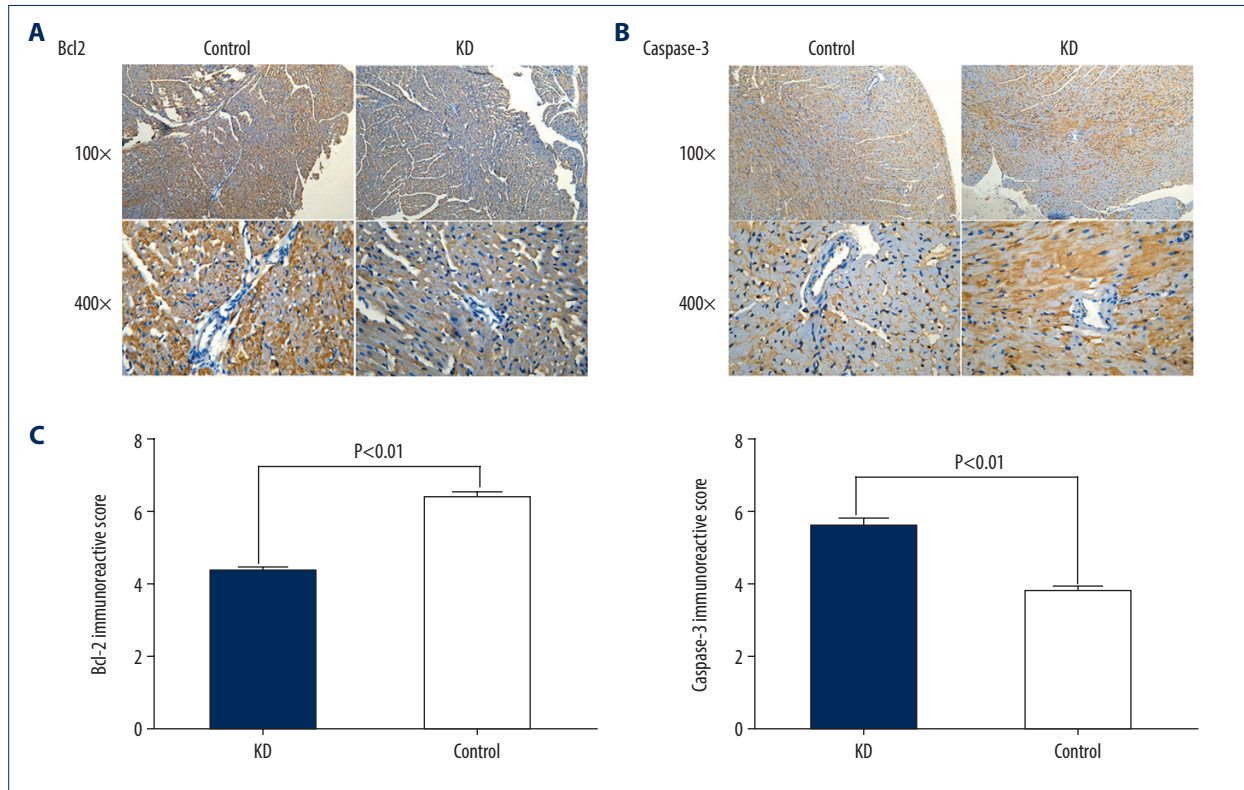


**Figure 3.** Comparison of Bcl2 (A, C) and caspase-3 (B, C) IRS values between the KD (n=12) and control groups (n=12). Comparison of Bcl2 (A) and caspase-3 (B) IRS values in the KD group and control groups. Cytoplasmic staining of Bcl2 in CASMCs was mild in mice of the KD group but was strong or moderate in mice of the control group (A). Cytoplasmic staining for caspase-3 in CASMCs was strong and moderate in mice of the KD group but mild or absent in mice of the control group (B). The IRS values for Bcl2 and caspase-3 were significantly different between the KD group and the control group (C).

cells (n=2) in the control group. Cytoplasmic staining for caspase-3 in CASMCs was strong in 75% of mice (n=9) and moderate in 25% of mice (n=3) in the KD group compared with mild staining in 33.33% of mice (n=4) and no staining in 66.67% of mice (n=8) in the control group. The Bcl2 and caspase-3 IRS values in the KD group were  $4.43\pm 0.51$  and  $5.60\pm 0.50$ , respectively, compared with  $6.37\pm 0.765$  and  $3.83\pm 0.38$  in the control group, respectively ( $t=5.79$  and  $5.24$ ;  $P$  all=0.001; Figure 3, Table 1). In sum, these findings show that Bcl2 expression was downregulated in the coronary artery of KD vasculitis mice compared with control mice, whereas the opposite change in caspase-3 expression was observed.

We also examined the correlation of the expression of p53 and p21 with caspase-3 expression. As shown in Figure 4, Pearson correlation analysis revealed that the IRS for caspase-3 was positively correlated with the IRSs for p53 and p21 in the KD group ( $r=4.67$  and  $4.83$ ; all  $P<0.001$ ).

#### Determination of predictive abilities of p53, p21, and caspase-3 for the development of CASMC apoptosis

ROC curves were used to determine the values of p21, p53, and caspase-3 expression for predicting the development of CASMC apoptosis and CAL formation in KD vasculitis mice. As

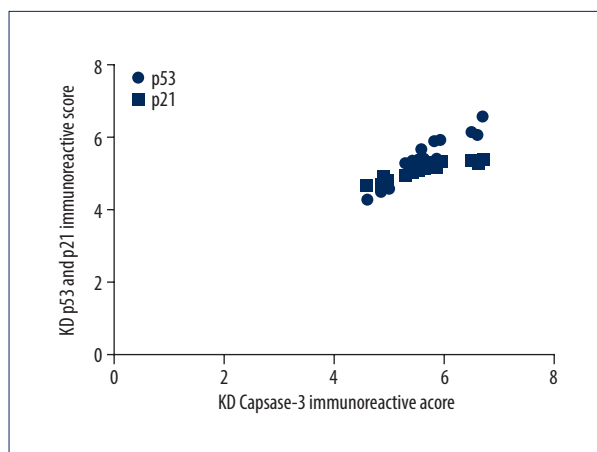


**Figure 4.** Correlation of p53 and p21 IRS values with the caspase-3 IRS in the KD group. Pearson correlation analysis revealed that the IRS for caspase-3 was positively correlated with the IRSs for p53 and p21 in the KD group ( $r=4.67$  and  $4.83$ ; all  $P<0.001$ ).

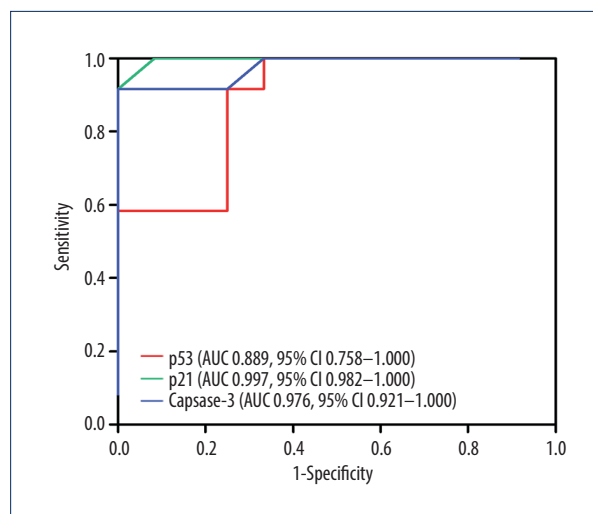


**Figure 5.** Comparison of ROC curves for p53, p21, and caspase-3 in all KD vasculitis mice with CALs. The AUC values and 95% CIs for p53, p21, and caspase-3 expression. The optimal cutoff values for p53, p21, and caspase-3 expression were 4.15, 4.18, and 4.22, respectively.

**Table 2.** Determination of predictive abilities of p53, p521 and caspase-3 IRS values for CASMC apoptosis in KD mice.

Parameter	p53 IRS	p21 IRS	Caspase-3 IRS
AUC	0.889	0.997	0.976
95% CI	0.758–1.000	0.735–1.000	0.615–0.998
Sensitivity	0.917	1.000	0.917
Specificity	0.750	0.917	1.000
Positive likelihood ratio	11.6	12	11.8
Optimal cut-off, score	4.15	4.18	4.22

shown in Figure 5 and Table 2, the AUC values for p53, p521, and caspase-3 expression were 0.889, 0.997, and 0.976, respectively. Also, the 95% CIs for these factors were 0.758–1.000, 0.735–1.000, and 0.615–0.998, respectively. In addition, p53, p521 and caspase-3 had sensitivity values of 91.7%, 100%, and 91.7%, respectively, and specificity values of 75%, 91.7%, and 100%, respectively. The optimal cutoff values for p53, p21, and caspase-3 expression were 4.15, 4.18, and 4.22, respectively, with high positive likelihood ratios of 11.6, 12.0, and 11.8, respectively. Collectively, these findings suggest that p53, p21, and caspase-3 expression may serve as a valid predictor of CASMC apoptosis and Cal formation in KD vasculitis mice.

## Discussion

In this study, we compared the apoptosis observed in the root of the coronary artery between KD vasculitis mice and control

mice and examined the related molecular basis. We found that KD vasculitis mice had increased apoptosis in the coronary artery, which was coincident with the increased expression of p21, p53, and caspase-3 and decreased expression of Bcl-2. Also, we found a significant correlation of p53 and p21 expression with caspase-3 expression. Moreover, we uncovered the predictive values of p53, p21, and caspase 3 expression for development of apoptosis as well as CALs in KD vasculitis mice.

Currently, the pathological mechanisms leading to CASMC apoptosis and CAL formation in KD are not completely understood. Further, the relationship between CASMC apoptosis and p53, p21, and caspase-3 expression has not been investigated, although some studies examined the apoptosis of vascular SMCs. For example, Lopez-Candales et al. [7] reported that the main pathological feature of AAA was SMC apoptosis, which was related to p53 overexpression. Therefore, it was speculated that p53 may be a marker of SMC apoptosis [7]. Wang et al. [15]

showed that p53 induces growth arrest and apoptosis in human vascular SMCs, with p53 directly regulating the transcription of p21, and p21 activation leading to cell apoptosis. Conversely, the expression level of p21 also reflects the activity of p53. When the expression of the variant p21 is increased, the activity of p53 is enhanced, which is pro-apoptotic [16]. Although p21 is a well-documented cell cycle regulator, it is also a regulator of DNA repair in apoptosis and acts downstream of p53 [16,17]. In line with these findings, in this study, inflammation and necrosis were observed in the coronary artery roots of KD vasculitis mice, and the number of apoptotic CASMCs was significantly increased along with increased expression of p53 and p21. Our study also showed a close relationship between upregulated p53 and p21 expression and CASMC apoptosis.

Bcl2 is an apoptosis-inhibiting factor with high expression in normal cells that is downregulated in some pathological conditions, such as ischemia-reperfusion injury and immune injury [8–10]. The mechanism by which Bcl2 suppresses apoptosis is via inhibition of the opening of the mitochondrial permeability transition pore (MPTP). The current study shows that Bcl2 was moderately or strongly expressed in the control group but mildly expressed in the KD group, indicating that Bcl2 was downregulated in the coronary artery of KD vasculitis mice [8–10]. Thus, decreased expression of Bcl2 is potentially implicated in the increased apoptosis of CASMCs and CAL formation in KD vasculitis mice.

The caspase family members are also well-recognized proapoptotic factors and have been found to play a role in CASMC apoptosis and mitochondrial-mediated apoptosis. Caspase-3 is usually present in cells in an inactive form (pro-caspase-3) that is converted to the active form by p53 and p21, which is a major marker of irreversible apoptosis [18]. The proapoptotic effects of p53 are mediated via several mechanisms, including activation of downstream target genes such as p21 and caspase-3, in which p53- and p21-dependent caspase-3 activation promotes CASMC apoptosis [18–20]. Mechanistically, activated caspase-3 interacts with poly ADP-ribose polymerase (PARP) to form cleaved PARP and induce cell apoptosis [9]. This study showed that caspase-3 was overexpressed in coronary artery

smooth muscle cells in KD vasculitis mice compared with control mice, in line with the observations of high p53 and p21 expression and elevated CASMC apoptosis. Combining our findings with previous studies, we believe that caspase-3 expression is closely associated with p53 and p21 expression.

In the present study, we also used ROC curve analysis to determine the performance of p53, p21, and caspase-3 expression in predicting CASMC apoptosis in KD vasculitis mice. We showed that all 3 factors exhibited high sensitivity and specificity and a positive likelihood ratio, supporting the notion that p53, p21, and caspase-3 may serve as valid predictors of CASMC apoptosis and CAL formation in KD vasculitis mice. Moreover, we also determined that the optimal cutoff values for the p53 IRS, p21 IRS, and caspase-3 IRS were 4.15, 4.18, and 4.22, respectively. Hence, these findings indicate that the expression levels of p21, p53, and caspase-3 hold diagnostic value for CAL formation in KD.

## Conclusions

In conclusion, our study demonstrated that the root of the coronary artery in KD vasculitis mice exhibits increased apoptosis, which is accompanied by upregulated expression of p53, p21, and caspase-3 and downregulated expression of Bcl2. The ROC curve analysis revealed that p21, p53, and caspase-3 may hold diagnostic value for CAL formation in KD, as upregulated expression of p21, p53, and caspase-3 promotes apoptosis of CASMCs.

## Statement

The funder had no role in study design, data collection and analysis, decision to publish, or preparation of the manuscript.

All surgeries were performed under sodium pentobarbital anesthesia, and all efforts were made to prevent suffering.

## Conflict of interests

None.



## References:

1. Yorifuji T, Tsukahara H, Doi H: Early childhood exposure to maternal smoking and Kawasaki disease: A longitudinal survey in Japan. *Sci Total Environ*, 2019; 655: 141–46
2. Singh S, Jindal AK, Pilania RK: Diagnosis of Kawasaki disease. *Int J Rheum Dis*, 2018; 21: 36–44
3. Denby KJ, Clark DE, Markham LW: Management of Kawasaki disease in adults. *Heart*, 2017; 103: 1760–69
4. Pinna GS, Kafetzis DA, Tselkas OI et al: Kawasaki disease: An overview. *Curr Opin Infect Dis*, 2008; 21: 263–70
5. Nakamura Y, Yashiro M, Uehara R et al: Increasing incidence of Kawasaki disease in Japan: Nationwide survey. *Pediatr Int*, 2008; 50: 287–90
6. Thissen JB, Isshiki M, Jaing C et al: A novel variant of torque teno virus 7 identified in patients with Kawasaki disease. *PLoS One*, 2018; 13: e0209683
7. Lopez-Candales A, Holmes DR et al: Decreased vascular smooth muscle cell density in medial degeneration of human abdominal aortic aneurysms. *Am J Pathol*, 1997; 150: 993–1007
8. Dejean LM, Martinez-Caballero S, Guo L et al: Oligomeric Bax is a component of the putative cytochrome c release channel MAC, mitochondrial apoptosis-induced channel. *Mol Biol Cell*, 2005; 16: 2424–32
9. Shalini S, Dorstyn L, Dawar S et al: Old, new and emerging functions of caspases. *Cell Death Differ*, 2015; 22: 526–39
10. Liu H, Jing X, Dong A et al: Overexpression of TIMP3 protects against cardiac ischemia/reperfusion injury by inhibiting myocardial apoptosis through ROS/Mapks pathway. *Cell Physiol Biochem*, 2017; 44: 1011–23
11. Gao L, Fu S, Wang W et al: Notch4 signaling pathway in a Kawasaki disease mouse model induced by *Lactobacillus casei* cell wall extract. *Exp Ther Med*, 2017; 13: 3438–42
12. Yeung RS: Lessons learned from an animal model of Kawasaki disease. *Clin Exp Rheumatol*, 2007; 25: S69–71
13. Wullschlegler S, Loewith R, Hall MN: TOR signaling in growth and metabolism. *Cell*, 2006; 124: 471–84
14. Lin ZY, Huang YQ, Zhang YQ et al: MicroRNA-224 inhibits progression of human prostate cancer by downregulating TRIB1. *Int J Cancer*, 2014; 135: 541–50
15. Wang X, Zou Y, Sun A et al: Emodin induces growth arrest and death of human vascular smooth muscle cells through reactive oxygen species and p53. *J Cardiovasc Pharmacol*, 2007; 49: 253–60
16. Kaija HM, Sarkioja T, Kortelainen ML et al: Stress-specific responses of p21 expression: Implication of transcript variant p21 alt-a in long-term hypoxia. *J Cell Biochem*, 2012; 13: 544–52
17. Fernandez-Majada V, Welz PS, Ermolaeva MA et al: The tumour suppressor CYLD regulates the p53 DNA damage response. *Nat Commun*, 2016; 7: 12508
18. Chan KM, Rajab NF, Siegel D et al: Goniothalamin induces coronary artery smooth muscle cells apoptosis: The p53-dependent caspase-2 activation pathway. *Toxicol Sci*, 2010; 116: 533–48
19. Cubillos-Rojas M, Schneider T, Bartrons R et al: NEURL4 regulates the transcriptional activity of tumor suppressor protein p53 by modulating its oligomerization. *Oncotarget*, 2017; 8: 61824–36
20. You BR, Park WH: Proteasome inhibition by MG132 induces growth inhibition and death of human pulmonary fibroblast cells in a caspase-independent manner. *Oncol Rep*, 2011; 25: 1705–12